The Golden Section: A Cosmic Principle

THEODOR LANDSCHEIDT

Previously published in Considerations X: 1

QUESTIONS:
Recent studies have confirmed that the cure of a breast tumor by surgery is dramatically more likely around the 17th day after the beginning of the patient's menstrual period than it is at other times in the menstrual cycle (Hrushesky, 1994). For what reasons?

Conception just in the middle of the ovulation cycle gives an 85% chance of a boy, whereas conception on the 10th day of the cycle is linked to an 87% chance of a girl (Thumshirn, 1975). On what account?

Why has the 11-year sunspot cycle just this length?

Why is the mean period of the secular cycle of sunspot activity—a main factor in climatic change—just 89 years?

Scientists have found significant cycles in rainfall linked to the lunation cycle, but not to the cardinal phases of the Moon. How can we account for this?

Why is it that the "plus zones" in the diurnal circle found by Michel Gauquelin do not fall on the cardinal points of the diurnal circle, but in between and not even symmetrically?

Why does the "Gauquelin effect" not include the Sun, Mercury, and the planets beyond Saturn?

What are there phase reversals in solar-terrestrial cycles that are in the way of dependable predictions?

Scientists and astrologers have found no convincing answers to these questions and many similar ones. Yet it is not unachievable to solve all of these problems. We only have to look without any preconceptions at the dynamics of the solar system, at the cosmic dance performed by the Sun and planets.

Five-Fingered "Hands " in the Sun's Dynamics

Figure 1 shows a strange cycle many astronomers and most astrologers do not know of. It is formed by the Sun's oscillations about the invisible center of mass of the solar system. Newton described this dynamic process three hundred years ago. The small open circles indicate the celestial positions of the system's center of mass relative to the Sun's

Figure 1: Master cycle of the solar system. Small circles indicate the position of the center of mass of the planetary system (CM) in the ecliptic plane relative to the Sun's center (cross) for the years 1945 to 1995. Heliocentric representation and marking the limb of the Sun make it easy to see whether CM is above or below the Sun's surface. The Sun's center and CM can come close together, as in 1951 and 1990, or reach a distance of more than two solar radii. Between these two extremes, the Sun's orbital angular momentum can increase or decrease forty-fold.

center, marked by a cross, for the years 1945 to 1995. The large solid circle marks the Sun's surface. Most of the time, the center of mass is to be found outside of the Sun's body. Intriguingly, the Sun's rather irregular oscillatory motion is regulated by constellations of the giant planets Jupiter, Saturn, Uranus and Neptune. Conjunctions and oppositions have the strongest impact. When Jupiter, Saturn, Uranus and Neptune form a more or less wide conjunction, the Sun's center and the center of mass are wide apart; they can reach a distance of more than two solar radii. When Jupiter alone opposes Saturn, Uranus and Neptune on the other

side of the Sun, the two centers come close to each other. Sometimes they make a very close approach as in 1951 and 1990. In the Sun's irregular cyclic motion between these two extremes its orbital angular momentum can in-crease or decrease 40-fold. If there is transfer of orbital angular momentum to the Sun's spin momentum—and there is evidence of it—this can affect solar activity. I have

shown that special planetary constellations linked to crucial change in the Sun's orbital momentum make it possible to predict solar-terrestrial events dependably. Thus my forecasts of energetic solar eruptions and geomagnetic storms, checked by astronomers and the Space Environment Services Center in Boulder, achieved a hit rate of 90% though the predicted events show a very irregular distribution. As to details, I refer to my book *Sun-Earth-Man* (Landscheidt, 1989). I also forecast the end of the Sahelian drought three years in advance (Landscheidt, 1983).

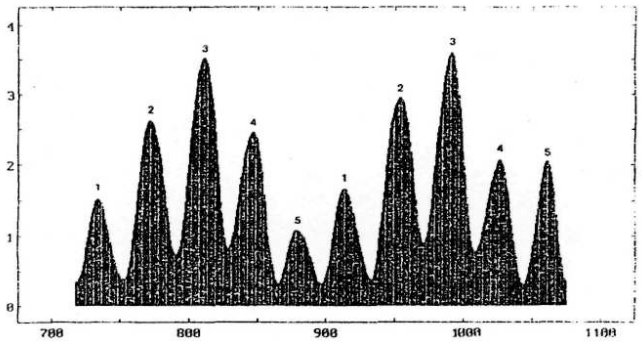

Figure 2: The Sun's dynamics displays five-fold symmetry, thought to be reserved to the realm of life. "Big hands" with "big fingers" emerge, when the 9-year running variance *of* the Sun's orbital angular momentum is plotted. Big hands and big fingers cover cycles o/solar activity with mean lengths *of* 178.8 years and *35.8* years, which are reflected in terrestrial cycles

The dynamics in the Sun's motion around the center of mass can be defined quantitatively by the change in its orbital angular momentum. The rate of change is usually measured by derivatives. In some respects the running variance yields more informative results. It applies the well-known smoothing technique of running means over two, three, or more consecutive readings to a running variance, the square of the standard deviation.

Figure 2 shows the 9-year running variance of the Sun's orbital angular momentum for the years 720 to 1070. And what does it reveal? "Big hands" with "big fingers"! These five-fingered hands were an utter surprise to me when I saw them first on my computer screen. Scientists conceive that the Sun is a body of "dead" matter. As such the Sun should not display five-fold symmetry. Two-fold, three-fold, four-fold, or six-fold symmetry like crystals, but not five-fold symmetry reserved to the realm of biology. I realized at once that the unexpected pentadactyl pattern was hard evidence of the fact that the Sun's dynamics and life forms on Earth are subjected to the same structural laws. This unexpected extension of the domain of five-fold symmetry to the realm of "dead" matter is all the more important as planets and their constellations are involved in the generation of the pattern governed by the number five presented in Figure 2.

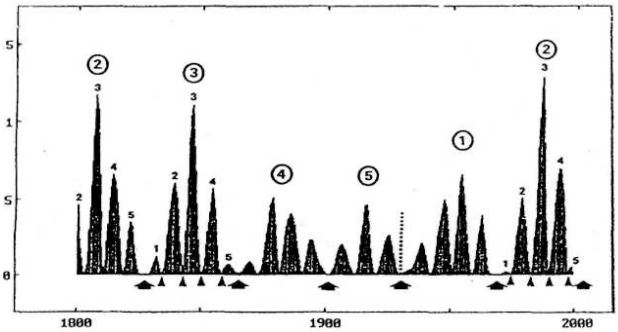

Figure 3: A fractal pattern in the Sun's dynamics. "Small hands" with "small fingers" appear within big fingers, when the 3-year running variance of the Sun's orbital angular momentum is pictured. Big encircled numbers mark the tips of big fingers. Small fingers below are indicated by small numbers. Big arrows and small triangles designate the start of big and small fingers respectively. Small fingers are related to solar-terrestrial cycles of shorter length. The vertical dotted line marks the initial phase (1933) of a big hand. This nodal point coincided with the establishment of Stalin's and Hitlers dictatorship and the Great Depression.

Fractals Generated by Cosmic Bodies

Closer examination reveals that there is even more to this pattern. A ubiquitous note in present day science is the term fractal coined by B. B. Mandelbrot (1983) in his work *The Fractal Geometry of Nature.* He stressed that clouds are not spheres, mountains are not cones, and lightning does not travel in a straight line. A fractal can be defined as a geometrical shape whose structure is such that magnification or reduction by

a given factor reproduces the original object. Self-similarity on different scales is a preeminent feature of fractals. A good paradigm is an unending sequence of Russian dolls, one nestled inside the other. Fractal substructures become visible by amplification. The Nobel Prize-recipient Wilson has shown that renormalization transformations involving a change of scale can serve as a universal tool in research. If you do not get ahead in your research, choose a coarser or a finer scale.

Figure 3 is the result of an amplification of the pattern in Figure 2. It shows the 3-year running variance of the Sun's orbital angular momentum. I was astounded when I first saw that there are fractals in the Sun's motion. The big fingers in big hands contain small hands with small fingers. The big encircled numbers at the top mark the tips of big fingers. The small fingers below are indicated by small numbers. Big arrows and small triangles at the bottom designate the starts of big and small fingers respectively. The vertical dotted line labels the start of a big hand in 1933.

It should be noted in passing that this dynamically fundamental period coincided with the establishment of Stalin's and Hitler's dictatorship and the Great Depression. The preceding start of a big hand in 1756 was again a crucial period. The Seven Year's War in Europe gave Great Britain as an ally of Prussia the opportunity to establish its Empire by the conquest of India and Canada. In my book *Sun-Earth-Man* I have given an explanation why the Sun's dynamics, regulated by the planets, has an effect on human behavior.

Cycles Linked to the Sun ʳs Pentadactyl Pattern

Big hands (BH), big fingers (BF), and small fingers (SF) are not only of theoretical importance. As I have shown, they represent distinct cycles of solar activity that are a paramount factor in solar-terrestrial relations (Landscheidt, 1983, 1986, 1987, 1990, 1994a, 1994b). The mean lengths of these cycles (C) are as follows: BHC = 178.8 years; BFC = 35.8 years; SFC = 7.2 years. These periods are rounded mean lengths. The real cycles differ in width. Yet all these variations can be computed and predicted from planetary positions and constellations. All of these cycles are fractals with subcycles. Especially half cycles play an important role. Half a big hand (HBHC = 89.4 years) represents the secular Gleissberg-cycle of sunspot activity which modulates the amplitudes of the well-known 11-year sunspot cycle and shows a narrow correlation with climatic change (Friis-Christensen and Lassen, 1991). Half a big finger (HBFC = 17.9 years) is an important factor in climate. I could show that maxima in the Lake Saki varve thickness are consistently correlated with consecutive HBF's (Landscheidt, 1990). Varves are banded layers of silt and sand deposited annually in lakes. The thickness of Lake Saki varves is related to local precipitation: the thickest varves are linked to very wet years and the thinnest varves to very dry years. The analysis covers data from A.D. 700 to 1894.

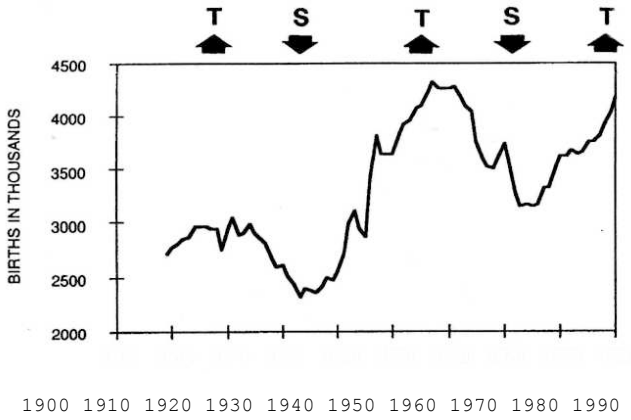

Figure 4: Annual birth rates in U.S.A. since 1909, after Poire (1994)

Figure 4, from N. Pont (1994), demonstrates that HBFC's are also to be found in man. It shows annual birth rates in the U. S. A. since 1909. The U.S. population does not increase at a steady linear rate, but fluctuates in a big-finger pattern. The starts of big fingers (BFS or S) go along with minima and big finger tips (T) with maxima in the birth rates. The next bottom in the U.S. population cycle is to be expected around 2007, the next BFS. Half small fingers (HSFC = 42 months) are connected, among other relationships, with a well-known cycle in stock prices.

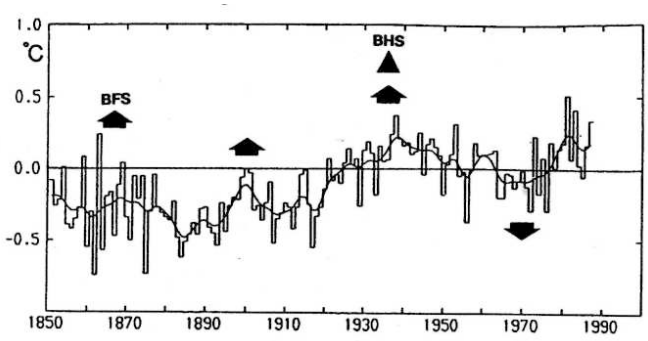

Figure 5: Annual-mean surface air temperature averaged over the Northern Hemisphere from 1850 to 1987, after Jones (1988).

Big and Small "Fingers": A Hierarchical Structure

The fractal of hands and fingers has a hierarchical structure. It offers a solution of the seemingly untractable problem of phase reversals in cycles. Figure 5, from P. D. Jones (1988), presents an example. It shows the time series 1850 to 1987 of the annual-mean surface air temperature averaged over the Northern Hemisphere.

The arrows, I added, designate the starts of big fingers (BFS) that fall in the data range. The BFS's 1867, 1901 and 1933 coincide with outstanding temperature maxima, as indicated by the smoothed curve. The BFS 1968, however, indicates the bottom of a downtrend that began after BFS 1933. Obviously, this is due to a phase reversal in the BFS pattern. We have learnt from experimentation with electrical and mechanical control equipment that at nodal points, where the response of the system is zero, the phase can shift by 180° (Burroughs, 1992). The start of a big finger is such a nodal point. Yet it is crucial that the BFS 1933 is at the same time the start of a big hand (BHS). In Figure 5, BHS 1933 is marked by a filled triangle. Such nodal points higher up in the hierarchy of cycles in the Sun's dynamics are dominant and can induce phase reversals in subordinated cycles as demonstrated in this case. As the next start of a big hand will not occur before 2111, the epoch of the coming BFS in 2007 should go along with another bottom in the surface air temperatures.

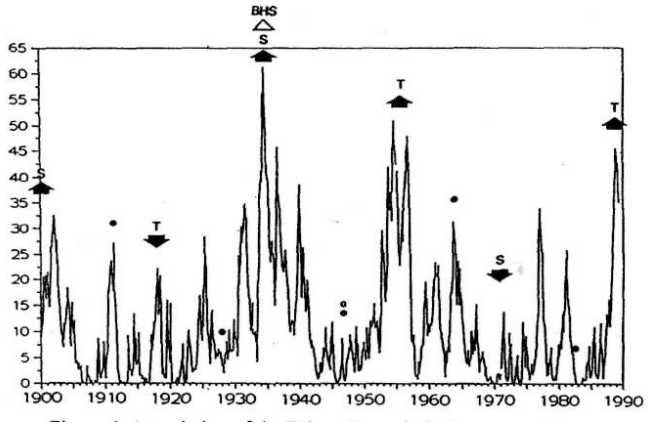

Figure 6: Association of the Palmer Drought Index, measuring the percentage of area covered by drought, with epochs of BFT's and BFT's, marked by arrows and indicators for start (S) & tip (T).

Another example from a wealth of inexhaustible relationships is presented in Figure 6. It shows the plot of the Palmer Drought Index for the U.S. from 1900 to 1989. The vertical axis measures the percentage of area covered by drought. Here big finger tips (BFT) come in, which represent maxima in the running variance of the Sun's orbital angular momentum. The arrows mark consecutive epochs of BFS's and BFT's. Up to 1933, the starts of big fingers (S) coincided with drought maxima and the tips (T) with minima. After the BHS 1933, indicated by an open triangle, the correlation with BF phases continued, but a phase reversal changed the rhythmic pattern. Now BFTs coincided with drought peaks and BFS's with bottoms. The new rhythm has been stable since 1933. So there is a good chance that it will continue till the next BHS in 2111. For some years around the next BFS epoch 2007, farmers in the U.S. should expect a wet climate. Up to now, both science and astrology have not been able to solve the problem of long-range drought prediction with their special means. Only when their faculties are united in a genuine interdisciplinary approach do solutions emerge that were not accessible before.

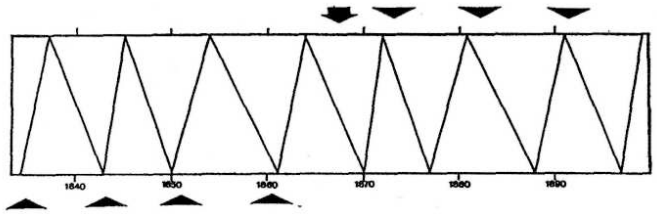

Figure 7: Cycle in U.S. pig-iron prices 1834 to 1900, after Dewey

There is also convincing evidence that big fingers are dominant in relation to small fingers. Figure 7 from E. R. Dewey shows the response to a cycle in U. S. pig-iron prices. Flat triangles indicate the epochs of SFS's. The big arrow marks the BFS in 1867 that resulted in a phase reversal in the time series. Before 1867 SFS's coincided with bottoms in the prices and afterwards with peaks.

Figure 8, after E. R. Dewey (1973), presents the percentile deviation of U.S. stock prices from the 9-year moving average trend, from 1830 to 1942. Flat triangles point to the epochs of SFS's that are related to ex-trema in the deviations. Fat arrows mark BFS's 1867 and 1933 which induced phase reversals. Before 1867 SFS's coincided with bottoms in the stock prices. After 1867 this pattern changed and SFS's went along with price peaks. The BFS 1933 induced another reversal, and SFS's again linked to bottoms in stock prices. After the BFS 1968 all deep international bottoms in stock prices—1970, 1974 and 1982—were closely connected with SFS's. This is why I had been predicting for years the

next worldwide deep bottom in stock prices would occur in 1990. I wrote: "Because of the imminent ... event (SFS), the epoch of which is 1990.3, a bottom may be expected such as occurred in 1970, 1974, and 1982. But this will also be the start of a new rally." (Landscheidt, 1989). Both of these came about, the international bottom in stock prices and the ensuing rally with new record highs. The next worldwide bottom is to be expected in 1998, the coming SFS epoch.

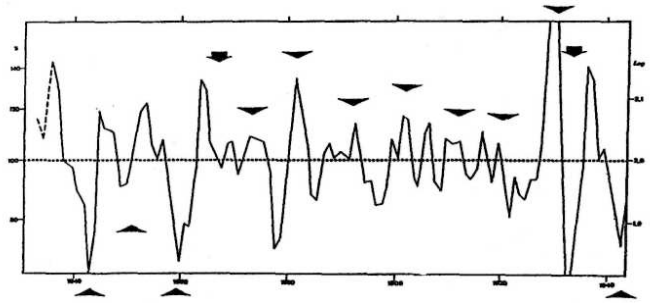

Figure 8: Percentage deviations of U.S. stock prices from the 9-year moving average trend for 1830 to 1942, after Dewey (1973).

The Number Five and the Golden Section

The fact that the Sun's dynamics are based on five-fold symmetry carries important information. The number five and the golden section are close relatives. Take a regular pentagon—a geometrical representation of the number five—and connect all of its corners by diagonals, as shown in Figure 9. A five-pointed star emerges, a pentagram, the intersecting lines of which form a web of golden sections. Within this star a new pentagon appears that contains a smaller star with golden section divisions, and so on, in an infinite fractal sequence. Literature that delves into this connection is widespread (Kappraff, 1991; Huntley, 1970; Landscheidt 1992, 1994a). Thus, there are indications that the pentadactyl pattern created by the Sun and the outer planets hints to a special function of the golden section in the solar system.

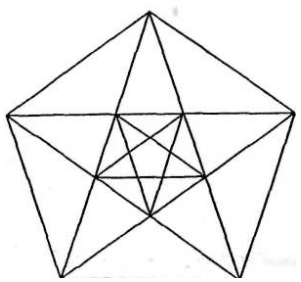

Figure 9: Five-fold symmetry, represented by a pentagon, shows intimate relationship with the Golden section.

Extrema within Cycles governed by the Golden Section

When I took the Sun's hints at the golden section seriously and discarded my blinders, I was suddenly able to realize that the golden section is not merely an aesthetic proportion important to artists, but an omnipresent cosmic principle that induces structural differentiation. The pro^ portions of the Greek temple in Figure 10 illustrate the golden section. It divides a frame structure like a line, a cycle, or any other delimited feature so that the ratio of the whole to the larger part—major —equals the ratio of the larger part to the smaller one—minor. Point G represents the golden number 0.618... This point divides the unit height of the temple into major (0.618...) and minor (0.3819...). To find the major of a line or cycle of any length, multiply it by 0.618. Multiplication by 0.382 yields the minor.

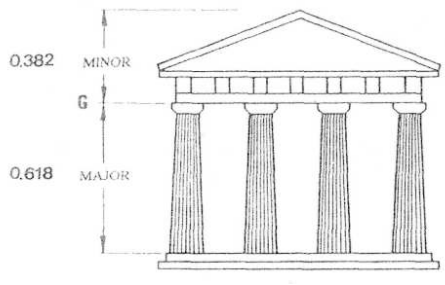

Figure 10: Proportions of a Greek Temple that illustrate the Golden Section

In mundane astrology we investigate cycles from one planetary conjunction to the next one, from new Moon to new Moon, and so forth. When we come across a sequence of outstanding maxima that emerge at reasonably regular intervals, we automatically think that we are dealing with crest phases of a cycle the ascending nodes of which precede the crests by 90°. We expect that special cosmic constellations should mark these zero phases. This inference, however, may be misleading. Cycles often possess inner structure that conspicuously deviates from the standard pattern of a sinusoidal wave marked by conjunction, opposition and squares.

Figure 11 presents an instructive example. The meteorologists D. A. Bradley, M. A. Woodbury and G. W. Brier (1962) investigated 16 056 heavy monthly rainfalls observed at 1,544 U.S. weather stations from 1900 to 1924 (solid line) and 1925 to 1949 (dashed line) and looked for correla-tions w,th the Moon's phases (marked at the bottom of the figure) The peaks of the patent cyclic pattern are statistically significant. Yet they show no direct connection with any of the lunar phases. Thus, most scientists dismiss a correlation between the lunar cycle and rainfall. Yet there is a conspicuous connection that is easy to see when we know how to look for the golden section. Within cycles from full Moon to full Moon and from new Moon to new Moon the rainfall maxima coincide with the major (0.618) of the golden section, whereas minima go along with the minor (0.382). The arrows, I added to the plot, point to this unexpected exact relationship between the extrema of the rainfall data.

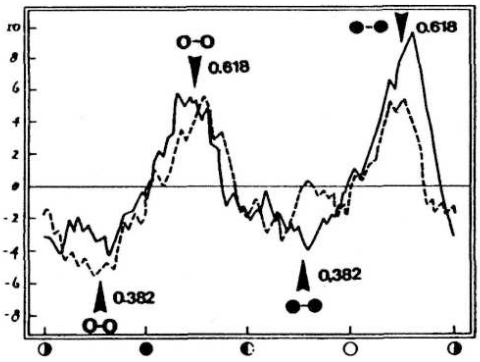

Figure 11: Heavy monthly rainfalls, observed at 1544 U.S. weather stations from 1900 to 1924 (solid line) and 1925 to 1949 (dashed line), after Bradley, Woodbury & Brier (1962).

Figure 12, after N. Kollerstrom (1984), shows a similar result.

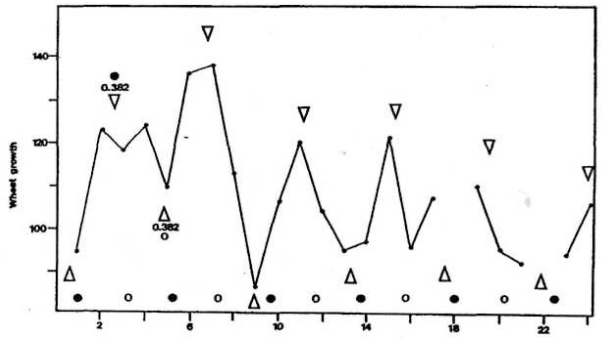

Figure 12: Yield of a heat germination study, after Kollerstrom (1984).

Figure 12 relates wheat germination to the synodic month, but shows no exact connection with new Moon or full Moon. In a 6-month study at Ewell Technical College, wheat seeds were germinated every Friday. Six days later they were removed and measured for germination and stem length. Temperature was kept constant. The curve in Figure 12 plots the measured total stem growth per batch of 25 seeds. The horizontal axis measures weeks. The data of the 18th and 22nd week were spoiled; so the curve shows interruptions at these points. New Moon and full Moon phases are marked at the bottom by filled and open circles. Minor sections (0.382) within the cycles from new Moon to new Moon are indicated by open triangles pointing downwards. They coincide with peaks in the data. Minor phases (0.382) phases within cycles from full Moon to full Moon are designated by open triangles pointing upwards. They go along with minima in the wheat growth. This relationship is all the more important as the results published by N. Kollerstrom are corroborated by wheat growth experiments performed by L. Kollisko (1936).

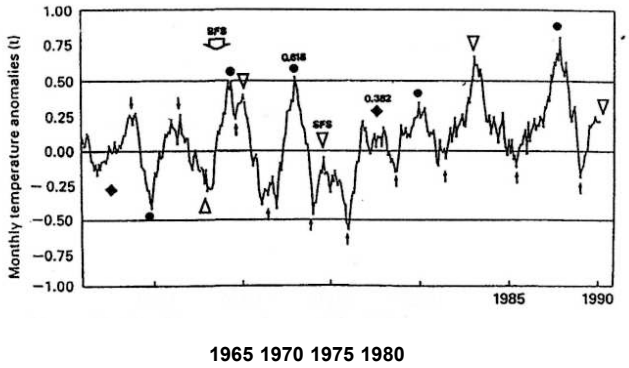

Figure 13: Monthly sea surface and land air temperature anomalies 1961-1989 for the tropical zone extending from 20N to 20S, after Houghton, Jenkins & Ephraums (1990). Strong peaks designate ENSO events (El Nino + Southern Oscillation), a cyclic large scale atmosphere-ocean interaction with climatic effects throughout the Pacific region and far beyond.

The connection presented in Figure 13, from J. T. Houghton, G. J. Jenkins and J. J. Ephraums (1990), solves a seemingly untractable problem of climatology and meteorology: the prediction of El Nino. It represents a cyclic large-scale atmosphere-sea interaction which has climatic effects throughout the Pacific region and far beyond. It is the only true global-scale oscillation that has been identified so far. This phenomenon is also called an ENSO event because of its links with the Southern Oscillation, a fluctuation of the intertropical atmospheric oscillation. Every three to seven years normally cold waters over the entire eastern equatorial Pacific Ocean show a dramatic warming of several °C which are associated with very large anomalies in global weather (Peixoto and Oort, 1992). The inhibition of the upwelling of nutrient-rich cold waters causes the death of a large proportion of the plankton population and a strong decline in the numbers of surface fish, especially anchovies. Birds and tuna, which depend on small fish for food, leave or die. The gas from decaying fish and birds is said to be so powerful that it can blacken the paint of ships passing by. These conditions do tremendous damage to the Peruvian economy.

The curve in Figure 13 plots the monthly sea surface and land air temperature anomalies 1961-1989 for the tropical zone extending from 20° N to 20° S. The stronger peaks indicate ENSO events. After the BFS 1968, marked by a big arrow, all SFS's, designated by open triangles, coincided with peaks in the plot. The same is true for all major sections (filled circles) within cycles formed by consecutive SFS's. In the case of SFC's longer than eight years, also the minor sections (filled diamond) went along with peaks. Troughs in the time series were rather exactly linked to midpoints (small arrows) in between consecutive crucial phases. Before the nodal phase of a big finger in 1968, the pattern was reversed. SFS's, as well

as majors and minors with small finger cycles, coincided with troughs, and the midpoints between these phases went along with peaks. The SFC running from SFS 1990.3 to SFS 1998.6 is longer than 8 years. Thus, the minor in 1993, the major in 1995, and the SFS in 1998 should coincide with peaks in the monthly temperature anomalies. As to 1993 this has become true already. The years 1995/1996 and 1998/1999 should see further positive temperature anomalies.

Now we may look back to Figure 6 to understand it entirely. The consecutive starts (S) and tips (T) form cycles of half big fingers within which the major (filled circles) alternatively points to maxima and minima in the drought covered areas. There is also a phase reversal in this pattern after the nodal point BHS 1933.

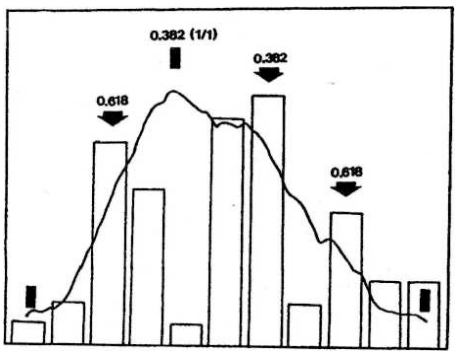

Figure 14:

Distribution of energetic solar eruptions within the 11 -year sunspot cycle, from EOS (1988).

Figure 14, from EOS (1988), presents an important case: the 11-year sunspot cycle. Its inner structure has been openly exposed to inspection by a legion of scientists and even some engaged astrologers, but no one has realized—as far as I know—that its maximum falls on a minor (0.382) of the golden section. So I bring a secret to light that has been patent all the time. It seems to be true: we are only able to see what we already know. Interestingly, the solar latitude around 35°, where Sun-spots first appear in a new cycle, is indicated by the minor of the distance from equator to pole. The bars in Figure 14 indicate the distribution of highly energetic solar eruptions within the 11 -year cycle. They are also related to the golden section. The sunspot cycle is a fractal; it comprises two sub-cycles: rise to maximum and fall to minimum. The strong eruptions concentrate on the major (0.618) of the rising part, and on the minor (0.382) and major (0.618) of the falling wing.

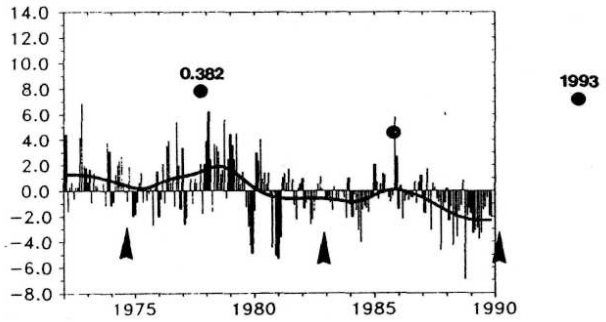

Figure 15: Changes in the snow cover of the Northern Hemisphere between January 1973 and March 1989, from Houghton, Jenkins & Ephraumis (1990)

Figure 15, from J. T. Houghton, G. J. Jenkins, and J. J. Ephraums (1990), shows the changes in the snow cover in the northern hemisphere between January 1973 and March 1989. SFS's are indicated by arrow heads. The minor (0.382) within SFC's is marked by filled circles. Minima in the snow-covered areas coincide with SFS's and relative maxima with minor sections. Around 1993—as could have been predicted from the pattern—the snow cover reached a maximum again. The next minimum is expected in 1998.

Now follows a rather complex example which corroborates our impression that Nature's imagination is more fertile than man's. Figure 16, from R. Mogey (1991), presents Wheeler's index of international battles. The data are structured by big finger cycles, the starts of which—1867, 1901, 1933, 1968, and 2007—are designated by triangles. Alternatively, these starting phases are related to minima and maxima in the number of

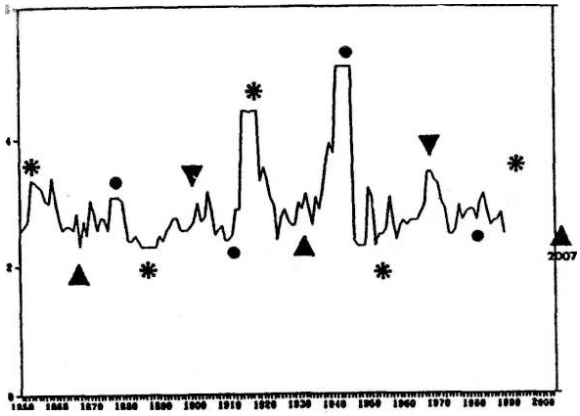

Figure 16: Wheeler's index of international battles, after Mogey (1991)

battles. The next minimum of this kind, a peaceful period, should develop around the year 2007. Now the golden section comes in. We take the lengths of the respective big finger cycles and subject them to the golden section so that we get two inner points, the distance of the minor from the big finger's starting-phase and the distance of the major from this start. In our plot, the minor points are marked by filled circles and the major points by stars. We get a consistent alternating pattern, as with the starts of the big fingers. In the first complete big finger cycle on the left, the minor (filled circle) coincides with a peak in battles and the major (star) with a trough. In the following cycle the relation is reversed. Now the minor points to a trough and the major to a large peak, the First World War. The next cycle shows another reversal. The minor coincides with the battles of the Second World War and the major with a trough in the index. The Gulf war and the war in Yugoslavia consistently coincide with the star on the right. The epoch of this major phase is 1992. We are still living within the range of effect of this active phase. I stressed this already at a conference of the Foundation for the Study of Cycles in Chicago in 1992. Meanwhile we have got Somalia, Rwanda, and Yemen. Further forecasting is easy. The next period of relative peace is to be expected around 2007, and the next war peak about 2021. These are rather special forecasts because we are dealing with specific time series. This is different from working with symbols.

Figure 17, from G. W. Brier (1967), shows rainfall, measured by U.S. stations, in relation to the lunar day from the Moon s lower culmination to the next one. We are interested in the subcycle designated by small arrows at the top. They run from lower transit to upper transit and from

upper transit to lower transit. The minor sections (0.382) within these subcycles are marked by fat arrows. They coincide with maxima in the precipitation data.

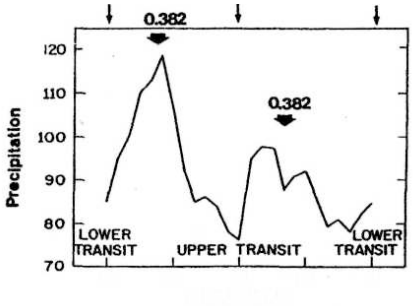

Figure 17: Rainfall and the lunar day (24.85 h), after Brier (1987)

0 6 12 18 O

LUNAR HOUR

Chronobiology—research in biological clocks and circadian rhythms —is a promising new field of science. Figure 18, from A. T. Winfree (1987), shows some results found in man. The displayed circadian rhythms run from midnight to midnight (O a- IC to O c IC). Start and restart of the respective cycles are marked by arrows.

About 10 minutes before 3 p.m. the threshold is higher by half. As can be seen in the bottom plots, at the same time numbness from anesthesia lasts several times longer than at night. So we ought to visit the dentist in the early afternoon, just at the time indicated by the major of the golden section, marked by triangles. The curve at the top right plots the retention of alcohol in the blood. It reaches a maximum in the morning just after 9 a.m., at the time of the minor. Implications for the practice of medication and drinking are obvious.

Golden Section and the Gauquelin Effect

In my book *Sun-Earth-Man* I have produced evidence that man's activity and even creativity is linked to the Sun's activity. Heliocentric constellations of planets are involved in this connection, as they regulate the Sun's activity via its oscillations about the center of mass of the solar system. When we apply our knowledge about the fundamental importance of the golden section without any prejudice, we find that it plays a vital role, too, in geocentric constellations of Sun, Moon and planets. For man, the day is one of the most important cycles. The biologist A. T. Winfree (1987) put it this was: "We live on a rotating planet. We grew up here. For three billion years, life here has grown and adapted, passing from cell to cell in-numerable times in unbroken descent, generation after generation. All the while, we have felt the sky brighten and darken again and again while the planet relentlessly rotated: a trillion cycles of brightness

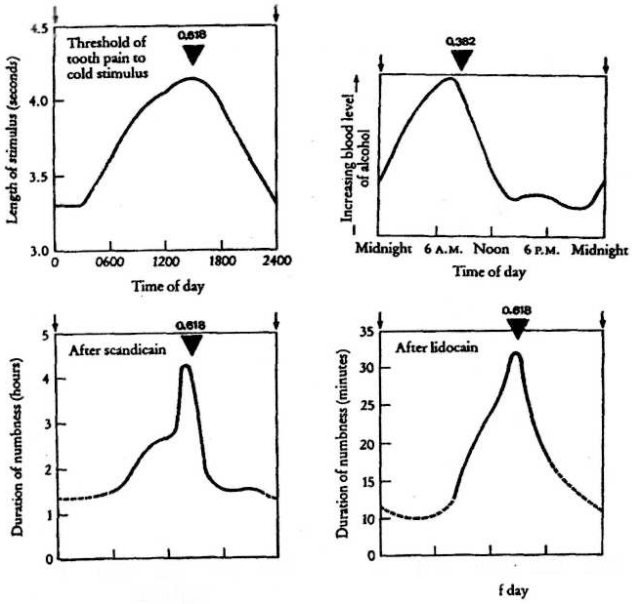

0 0600 1200 1800 2400 0 0600 1200 1800 2400

Time of day

Figure 18: Circadian rhythms in the Golden section, after Win-free (1987). Within cycles from midnight (q A IC) to midnight, marked by arrows, threshold of tooth pain and duration of numbness from scandicain or lidocain injection show a strong maximum at the major (0.618) of the Golden section, whereas the minor is linked to a maximum in retention of alcohol in the blood.

and dark, never missing a beat, always felt deep in the chemical essence of what we are. We are well adapted to the pervasive rhythm of Sunrise and Sunset." This is also true of the rising and setting of the Moon and planets.

Figure 19 shows a schematic representation of the diurnal circle. Sun, Moon and planets rise at R, reach upper culmination at UC, set at S, pass through the lower culmination at LC, and return to the rising point R. Actually, these are four cycles of different quality: from rising to the next rising, from upper culmination to upper culmination, from setting to setting, and from lower culmination to lower culmination. As these are real cycles that could have an inner structure, it is tempting to try what we get when we link individual birth times to the diurnal circle. The psychologist M. Gauquelin from the University of Paris was curious to do this. When he took the birth times of thousands of eminent professionals from

well-defined vocational groups and investigated the corresponding distribution of Sun, Moon and planets in the diurnal circle, he got a highly significant deviation from the expected random distribution as to Moon, Mars, Jupiter and Saturn, sometimes also Venus. The frequencies were considerably higher about one hour and a half after rising and upper culmination, and to a lesser degree at the opposite points. Though Gauque-lin s statistical work was state of the art and could be reproduced with new data, there was much criticism because the accumulations in the diurnal circle did not fall directly at or before the cardinal points rising, culmination and setting, but built up in between , and not even symmetrically. Yet I could show (Landscheidt, 1991) that the accumulations are exactly related to the cardinal points in the diurnal circle when the golden section is taken into ac-count.

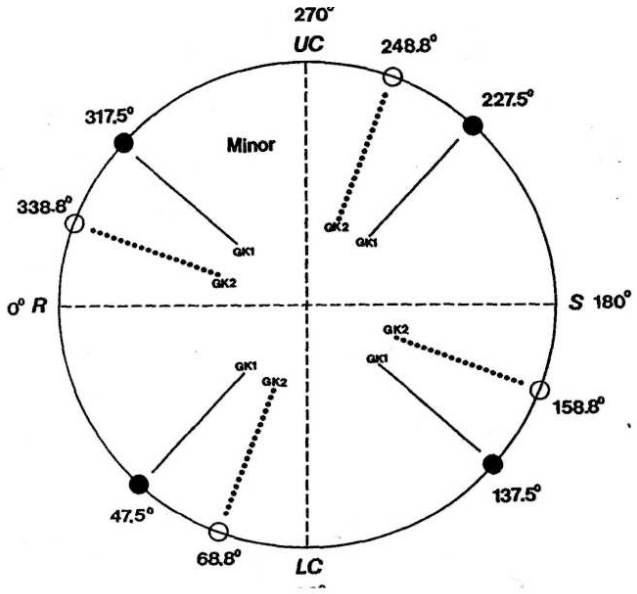

gcr *

Figure 19: Schematic representation of Golden section divisions within cycles formed by the rotating earth.

In our diagram, the origin of the diurnal circle of 360° is set at R, the rising point. We choose anti-clockwise direction, following the earth's rotation. To begin with, we look for the minor of the golden section in those four cycles we get, when we start from qualitatively different cardinal points. Multiplication of the circle of 360° by the minor 0.382 results in 137.5°. This is where we get when we start at the rising point R, the

origin 0°. The respective position is marked by a filled circle at the bottom right. Starting from LC, S, and UC results in 227.5°, 317.5° and 47.5°. We have only to add 137.5° to 90°, 180° and 270°. If we get a value greater than 360°, we have to subtract 360° to stay within the diurnal circle of 360°. The four minor positions, all designated by filled circles, form a cross, I call Golden Cross 1. As we have seen, cycles can be nested in cycles because they are fractals. The horizontal semicircles from rising to setting and from setting to rising have got different qualities as day and night. The vertical semicircles with celestial bodies ascending and descending are qualitatively different, too. Thus, we also calculate the positions of the minors in the four semicircles. We get the positions marked by open circles, which form Golden Cross 2. I was rather surprised when I saw that these golden crosses mark just those directions in the diurnal circle singled out by M. Gauquelin.

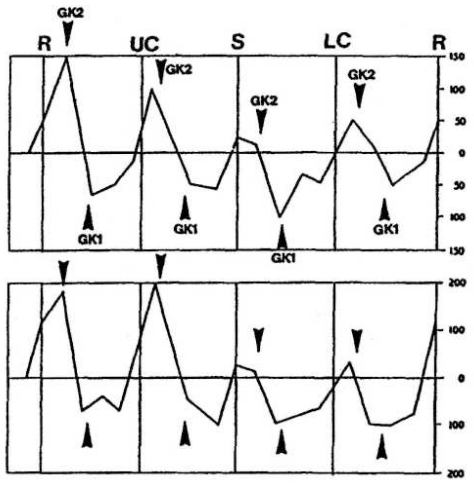

Figure 20: Linear representation of the diurnal circle of cf, \ +> and 5 at the birth times of 11,000 prominent French professionals (top) and 19,000 eminent professionals from Italy, Belgium, the Netherlands, and Germany (bottom), after M. Gauquelin (1960) and J. M. Addey (1976). The peaks in this distribution consistently coincide with Gold Cross 2 (GK2) and the bottoms with Golden Cross 1 (GK1),

Figure 20, after M. Gauquelin (1960) and J. M. Addey (1976), is a global, linear representation of Gauquelin's results. The curve at the top plots the positions of Mars, Jupiter, Saturn and Moon in the diurnal circle tor 11,000 birth times of prominent French professionals. The distribu-

tion for 19.000 birth times of eminent professionals from Italy, Belgium, the Netherlands, and Germany is plotted at the bottom. All of the peaks in both plots coincide with the directions in the diurnal circle indicated by Golden Cross 2 (GK2), whereas the bottoms go along with the sections of Golden Cross 1 (GK1). Arrows point to these crucial positions.

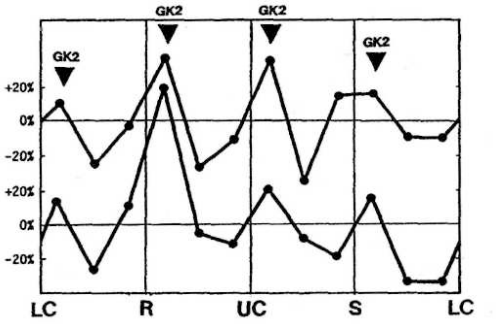

Figure 21: Mars distribution in the diurnal circle related to birth times of 2,299 famous sports champions (bottom) and 4,506 actors and scientists (top) with character traits similar to sports champions, after M. and F. Gauquelin (1976). All of the peaks fall exactly at sections of Golden Cross 2 (GK2), indicated by triangles.

The connection gets even more precise, when we isolate special planets and well-defined professional groups. In Figure 21, after M. and F. Gauquelin (1976), only the distribution of the planet Mars in the diurnal circle is shown. The distribution at the bottom was generated by the birth data of 2,299 sports champions. The plot at the top is related to the birth times of 4,506 scientists and actors with special biographies that stress character traits also found with successful sports champions. All of the maxima in the distributions fall exactly at the sections of Golden Cross 2 (GK2), indicated by arrows.

Figure 22, after M. Gauquelin (1973), presents the distribution of Mars for quite a different vocational group: 1,345 painters at the top, 703 musicians in the middle, and 824 writers at the bottom. These are typical artists. Their biographies shun character traits usually found with sports champions. There is a complete reversal in the connection with the golden section patterns. Golden Cross 1 (GK1) is now narrowly correlated with peaks in the distribution and Golden cross 2 (GK2) with valleys. Yet in some respects the groups differ. The musicians and writers show a connection with Golden Cross 4 (GK4) in different regions of the diurnal circle. This is a new feature that deserves special attention.

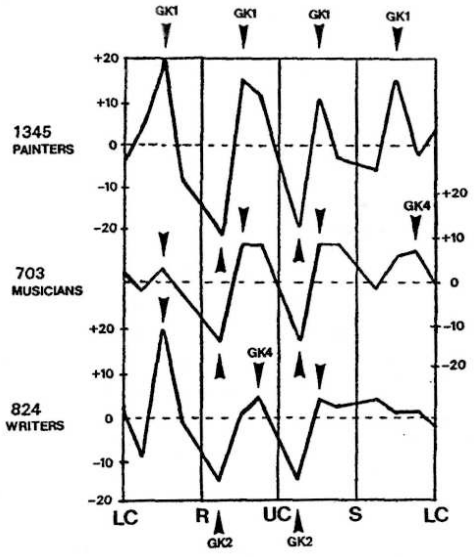

Figure 22: Diurnal Mars distribution based on the birth times of typical artists, after M. Gauquelin (1973). There is a reversal in the Golden section connections as compared to Fig. 20&21.

Sun, Mercury & the Outer Planets are Included

M. Gauquelin's results were queer in so far as he did not find any correlations for the Sun, Mercury, and the planets beyond Saturn. This was incompatible with astrological experience. As the Sun is by far the most massive body in the solar system and the dominant center of regulation, its absence in the relationship was rather unnatural. It seemed reasonable to assume that a solution of this problem

could be found by extending the golden section divisions of the diurnal circle to the major. Gold Crosses 3 and 4 emerge, when we divide the diurnal circle as before, but use the major instead of the minor of the golden section. Figure 23 shows the result. As expected, the further golden crosses close the gap.

In 1987 T. Shanks made a thorough investigation of the diurnal distribution of Sun, Moon and all planets based on the birth times of 10,464 eminent professionals from six vocational groups. He assessed the frequency of the ten investigated celestial bodies in 72 sectors of the diurnal circle and plotted the results for each body and each vocational group separately. The expected chance distribution was assessed by 50 control

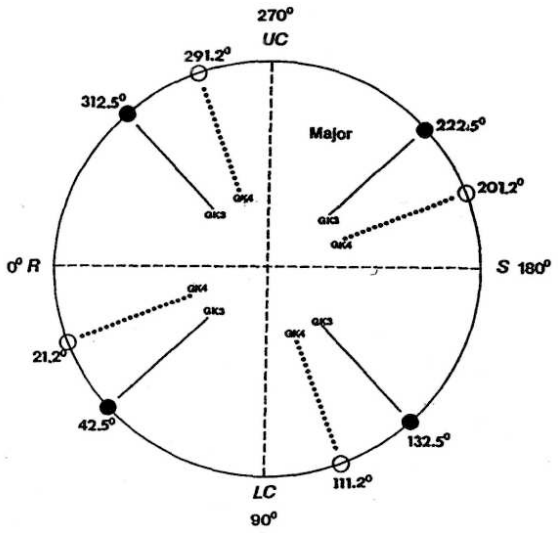

Figure 23: Schematic representation of Golden section divisions within cycles formed by the rotating earth as in Fig. 19, but based on the major (0.618) instead of the minor. The resulting Golden Crosses 3 (GK3) and 4 (GK4) are correlated with diurnal positions of O, 5 and planets beyond *> at the birth times of prominent professionals.

groups. The plots showed the deviations from these expected frequencies in the 72 sectors. The results were published at the 6th International Astrological Research Conference in London. From this material I selected the results for Sun, Mercury, Uranus, Neptune and Pluto. Then I chose for each of the five celestial bodies and each of the six professions the three strongest deviations from the expected frequencies and recorded how often they fell into 36 sectors of 10°. I obtained the distribution presented in Figure 24. It was subjected to a Gaussian low-pass filter.

The peaks alternatively conform with Golden Cross 3 (GK3) and Golden Cross 4 (GK4), derived from the minor. Out of 90 cases, 65 fall into 16 golden cross sectors and only 25 into the 20 sectors in between. A statistical evaluation of this distribution yields $x^2 = 28$ for 1 degree of freedom. The probability that this pattern is the result of chance is less than 1 in 6 million. This outcome is strong enough to support a working hypothesis that can serve as a base for further detailed investigations. Naturally, these results have to be checked by replications with new data. Yet it should be kept in mind that the upshot conforms with a wealth of other relationships with the golden section that are to be found in many different

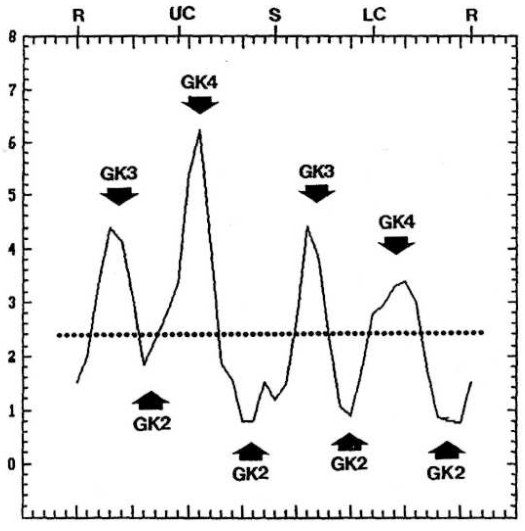

0° 50° *Wf* 15fl° 200° 23f 300° 350°

Figure 24: Special diurnal distribution of O, ?, %, Γ and E at the birth times of 10,464 eminent professionals from six vocational groups. Peaks consistently fall at Golden Crosses 3 and 4 (GK3 & GK4), and troughs at Golden Cross 2 (GK2)

Golden Aspects

The golden section divisions within cycles formed by the rotating earth may be considered a set of astrological aspects. The complete set emerges when we superimpose the two schematic diagrams in Figures 19 and 23, related to minor and major of the golden section, and compare all of those angles we find on the right and on the left of the origin

0°. Imagine that you are standing at the rising point R, or 0°, of the diurnal circle and are looking over to the setting point at 180°. Then the superimposed golden section divisions on your right form the set 21.25°, 42.49°, 47.51°, 68.75°, 111.25°, 132.49°, 137.51° and 158.75°. The angles 338.75°, 317.51°, 312.49° and so forth, on your left repeat the set on your right when subtracted from 360°. If we extend the fractal beyond the semicircle and include the quarter circle, the golden section operation generates the additional angles 34.38°, 55.62°, 124.38° and 145.62°. It is not an arbitrary procedure to divide cycles in halves and quarters. Obser-

vation shows that spectral peaks can appear at twice and four times the driving frequency, or at half or a quarter of it (Burroughs, 1992). Statistical tests indicate that the twelve golden aspects in the complete set are reliable.

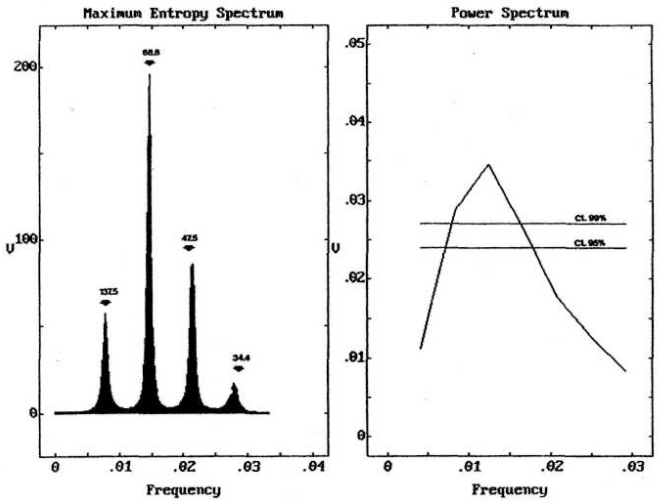

Figure 25: Angular separation of Sun and Galactic Center in birth charts of 600 celebrities. Results shown are from maximum entropy spectral analysis (plot on left) and Blackman-Tukey power spectrum (on right).

The result presented in Figure 25 shows that significant results can be achieved with relatively few cases. I took a sample of 600 celebrities from the German encyclopedia *Das kluge Alphabet* and measured the angular separation of Sun and galactic center. This makes sense as both of these elements are centers of regulation that are part of a cosmic hierarchy (Landscheidt, 1973). The left plot in Figure 25 shows the result of a maximum entropy spectral analysis of the distribution of the angular separations. The maximum entropy method—developed by J. P. Burg (1975)—is a new form of spectral variance analysis which shows much higher resolution than earlier methods, especially at lower frequencies. The four sharp peaks solely point to angles derived from golden section divisions: 137.5°, 68.8°, 47.5° and 34.4°. The plot on the right shows the Blackman-Tukey power spectrum (Blackman and Tukey, 1959). It is much coarser than the maximum entropy spectrum, but can be evaluated by special tests of significance. The first two peaks are well beyond the 99% confidence level. Similar investigations into 108 strong earthquakes, 132 heavy volcanic eruptions, 1,024 scientists, and 988 chief

executive officers have yielded highly significant results that corroborate the validity of the golden aspects, though in a more differentiated way than presented here. It would go beyond the frame of this paper to explain these additional results in detail.

According to my experience, the interpretation of golden aspects in individual charts and also the prediction of trends by means of golden transits yield practical results that go beyond the possibilities of traditional astrology. I shall delve into this complex topic in a special paper focusing on practice.

The Golden Section: A Principle of Nature

When we look back at the wealth of results that has yielded from our inquiry into the function of the golden section in diverse fields, the conclusion suggests itself that we are dealing with a principle of Nature. Modern research corroborates this inference. The golden section plays a central part in the KAM-theorem, developed by the mathematician A. N. Kolmogorov (1979), W. T. Arnold (1963), and J. Moser (1973). This theorem says that instability catastrophes in planetary systems can be prevented by planetary periods of revolution that form highly irrational quotients, whereas commensurable ratios—quotients formed by simple integers like 1 to 1, 1 to 2, 2 to 3, and so on—can induce resonance catastrophes by amplifications of disturbances. Mathematically, the golden number G is the most

irrational of all irrational numbers. Thus, the stability of planetary orbits, including the Earth's path, hinges on the golden section. Similarly, the physicist J. Greene (1979) provided proof that instability in plasma, the fourth state of matter, does not occur when quasi-periodic oscillations prevail that are governed by the golden section. In my book *Astrology: Hope of a Science?* I have shown that irrational and rational numbers, stability and instability, and, revealingly, the golden section and resonance configurations like conjunctions, oppositions and squares form a polarity, the poles of which represent opposite properties like close and open systems, geometry and algebra, asymmetry and symmetry, circle and straight line, female and male.

This can have far-reaching implications. It is well-known that there is a 28-day cycle of menstruation and ovulation which begins on the first day of menstrual period. Research published by the physician F. Benendo shows that the question: "boy or girl?" can be answered. Conception just in the middle of the cycle, at the time of ovulation, plus or minus one day, gives an 85% chance of a boy; whereas conception on the 10^{th} day of the cycle, plus or minus one day, is linked with an 87% chance of a girl (Thumshirn, 1975). Intriguingly, the 10^{th} day falls on the minor of the ovulation cycle of 28 days (28 multiplied by 0.382 is equal to 10.7). So the female sex shows a close relationship with the golden section and stability, whereas the male sex is exposed to instability, indi-

cated by the resonance ratio 1 to 2. No wonder that women have got a more stable health and live longer than men. Even mentally women are more stable. Yet there are always advantages and disadvantages.

Now we can understand, too, why on the 17^{th} day of the 28-day menstrual cycle the chance of a cure after breast tumor surgery is so much better than at other times in the cycle. The major of the 28-day cycle just falls at the 17^{tn} day (28 multiplied by 0.618 is equal to 17.3). Cancer is linked to disorder and instability. To fight it, the most stable phase in the menstrual cycle, the major section, seems to be best for a cure. Yet it should be taken into consideration that the menstrual cycle is an individual feature that can have different lengths in different women.

The Golden Section and the Length ofSunspot Cycles

At this point we are also in the position to answer the question asked at the beginning: Why has the 11 -year sunspot cycle just this length? We know that the stability of the planetary system hinges on the Golden section, which is intimately connected with five-fold symmetry that emerges in the Sun's dynamics, which again is related to the Sun's activity. Thus, it seems plausible to assume that main features of solar activity like sun-spot cycles are closely connected with the Golden section. This is so indeed. The real cycle of sunspot activity is the magnetic Hale cycle of 22.1 years. The Sun's global magnetic field varies over this period, during which the field reverses and is restored to its original polarity. One such Hale cycle comprises two successive 11 -year cycles with opposite magnetic polarities.

As we have seen, the mean interval covered by big fingers is 178.8 years + 5 = 35.76 years. The big finger cycle (BFC) of this length does not only show a high degree of correlation with the Gleissberg cycle that modulates the intensity of sunspot activity and climate on Earth, but also an exact relationship with the magnetic Hale cycle of 22.1 years and the sunspot cycle of 11.05 years. The golden number G = 0.618...—mathematically the most irrational of all irrational numbers—represents the golden mean. When multiplied by the length of the BFC, the exact Hale period emerges:

35.75 years [BFC] x 0.618 [G] = 22.1 years [Hale cycle]

The 22-year cycle is a dominant feature in the global record of marine air temperatures, consisting of shipboard temperatures measured at night (Burroughs, 1992), the detrended Central England temperature record of A.D. 1700 to 1900 (Mason, 1976), and the drought severity index covering different areas of Western United States (Mitchell, Stockton and Meko, 1979). R. W. Fairbridge & C. Hillaire-Marcel (1977) found evidence of the double Hale cycle in beach ridge formations going back to 8,000 B. C.

The exact length of the 11-year sunspot cycle appears, when multiplication by the golden number is applied to a half big finger (HBF):

17.88 years [HBF] x 0.618 [G] = 11.05 years [Sunspot cycle]

Thus, it becomes apparent that the length of the magnetic Hale cycle and of the 11-year sunspot cycle is connected with fivefold symmetry in the Sun's oscillations about the invisible center of mass of the solar system and the constellations of Sun and planets that generate it. We could also say that the length of these

important cycles of solar activity can be explained in astrological terms. Yet this aspect becomes accessible only when we follow Kepler, Galileo and Newton, who integrated astrological or alchemical imagination with methods and insights of modern science. Astrologers should acknowledge as well as scientists that we need a genuine interdisciplinary approach that combines the all-embracing astrological world-view with recent results in progressive science.

The more obvious 11-year sunspot cycle is much less prevalent in climatic data than the magnetic Hale cycle, though there are much more investigations looking for potential connections between the 11-year cycle and climate. The only solid link has been established by K. Labitzke and H. van Loon (1990). It correlates solar flux with quasi-biennial oscillation (QBO), 700 mb height and surface temperatures.

Further Connections

Those readers, who have been patient enough to come to this point will be able to see the Golden section anywhere in the cosmic environment. J. L. Lehman (1994), stimulated by findings of Project Hindsight, has drawn attention to a special Mars pattern in the diurnal cycle which emerges when births during the day are separated from births during the night. In both of the separated groups only one maximum and one minimum appeared in the distribution, but such that the maximum in one group matched the minimum in the other group, and vice versa. A Pearson test reveals that these patterns reach a much higher level of significance than the Gauquelin "plus zones". If J. L. Lehman had been aware of the cosmic function of the Golden section, she would have seen a close connection with golden aspects. The frequency distribution of day-born painters and musicians from the Gauquelin data shows a maximum close to 68.8° *after* rising, whereas the maximum of the night-born members of this group is near 68.8° *before* rising. Night-born politicians and actors show the same pattern. With military leaders and sports champions the maxima shifts from 68.8° to 111.3°. It should be noted that 111.3° and 68.8° represent the major and minor of a half circle of 180°. The two groups investigated by J. L. Lehman also result from a division into halves. This is only the rough picture. A closer examination

yields details that point to differences between the professional groups.

It would be interesting to deal with the frequency distribution of Moon, Venus, Mars, Jupiter and Saturn in the diurnal circle related to the birth data of 1,053 lesbians, presented by F. Schneider-Gauquelin (1993). Some of the most outstanding patterns that could explain lesbian inclinations astrologically are not linked to Gauquelin "plus zones" but to golden crosses. Yet this would go beyond the frame of this paper. 1 hope that those readers who are in resonance with the golden section will do investigations of their own.

References

Addey, J. M. 1976. *Harmonics in Astrology.* Romford: Fowler.

Arnold, W. I. 1963. Small Denominations and Problems of Stability of Motion in

Classical and Celestial Mechanics. *Russ. Math. Surv.,* 18, 85. Blackman, R. B., & J. W. Tukey. 1959. *The Measurement of Power Spectra.* New York:

Dover. Bradley, D. A., M. A. Woodbury, & G. W. Brier. 1962. Lunar Synodical Period and

Widespread Precipitation. *Science,* 137, 748. Brier, G. W. 1967. Rainfall and Lunar Tides. In *The Encyclopedia of*

Atmospheric Sciences and Astrogeology, ed. R. W. Fairbridge, 815. New York:

Reinhold.

Burg, J. P. 1975. Maximum Entropy Analysis. Ph. D. thesis. Stanford University. Burroughs, W. J. 1992. *Weather Cycles: Real or Imaginary?* Cambridge University

Press.

Dewey, E. R. 1973. *Cycles.* New York: Manor Books. EOS. 1988. *Transactions.* American Geophysical Union. Oct. 18, 1988. 1. Fairbridge, R. W., & C. Hillaire-Marcel. 1977. An 8000-Year record of the "Double-Hale" 45-Year Solar Cycle. *Nature,* 286, 413-416. Friis-Christensen, E., & K. Lassen. 1991. Length of the Solar Cycle: an Indicator of Solar

Activity Closely Associated with Climate. *Science,* 254, 698-700. Gauquelin, M. 1960. *Les hommes et les astres.* Paris: Denoel. —1973. *Die Uhren des Kosmos gehen anders.* Bern/Munich/Vienna: Scherz. Gauquelin, M., & F. Gauquelin. 1976. *The Planetary Factors in Personality.* Paris:

Laboratoire d'Etudes des Relations entre Rhythmes Cosmiques et

Psychologiques.

Greene, J. 1979. *Journal of Mathematical Physics. 20,* 1183. Houghton, J. T., G. J. Jenkins, and J. J.

Ephaums. 1990. *Climatic Change: The IPCC*

Scientific Assessment. Cambridge University Press.

Hrushesky, W. J. M., 1994. Timing is Everything. *The Sciences.* July/August, 1994, 36. Huntley, H. E., 1970. *The Divine Proportion. A Study in Mathematical Beauty.* New

York: Dover. Jones, P. D., 1988. Hemispheric Surface Air Temperature Variations: Recent Trends and

an Update to 1987.7. *Climate,* 1,645-660. Kappraff, J., 1991. *Connections. The Geometric Bridge Between Art and Science.* New

York: McGraw-Hill.

Kollerstrom, N., 1984. Wheat Germination and Lunar Phase. *Correlation, 4,* I, 25-31. Kollisko, L., 1936. *The Moon and the Growth of Plants.* London: Anthroposophical

Publishing Company. Kolmogorov, A. N., 1979. Preservation of Conditionally Periodic Movements With

Small Change in the Hamiltonian Function. *Lecture Notes in Physics,* 93, 51.

Labitzke, K. &H. van Loon. 1990. Association Between the 11-Year Sunspot Cycle.

the Quasi-Biennial Oscillation, and the Atmosphere: a Summary of recent

Work. *Phil. Trans. R. Soc.* London, A, 330, 577. Landscheidt, T., 1973. *Cosmic Cybernetics.* Aalen: Ebertin. —1983. Solar Oscillations, Sunspot Cycles, and Climatic Change. In *Weather and Climate Responses to Solar Variations,* ed. B. M. McCormac. Boulder: Colorado Associated University Press, 293-308.

—1986. Long Range Forecasts of Energetic X-Ray Bursts on Cycles of Flares. In *Solar-Terrestrial Predictions,* ed. P. A. Simon, G. Heckman, and M. A. Shea.

Boulder: National Oceanic and Atmospheric Administration, 81-89. —1987. Long Range Forecasts of Solar Cycles and Climatic Change. In *Climatic*

History, Periodicity, and Predictability, ed. M. R. Rampino, J. E. Sanders, and

L. Koenigsson. New York: van Nostrand Reinhold, 421-445. —1989. *Sun-Earth-Man: a Mesh of Cosmic Oscillations. How Planets Regulate Solar*

Eruptions, Geomagnetic Storms, Conditions of Life, and Economic Cycles.

London: Urania Trust. —1990. Relationship Between rainfall in the Northern Hemisphere and Impulses of the

Torque in the Sun's Motion. In *Climate Impact of Solar Variability,* ed. K. H.

Schatten and A. Arking. Proceedings of a conference held at NASA Goddard

Space Flight Center. Greenbelt: NASA Conference Publication 3086, 259-266. —1991. Der goldene Schnitt: ein kosmisches Prinzip [The golden section: a Cosmic

Principle]. *Meridian 1/92.* 37-41 and 2/92, 31-35. —1992. A Holistic Approach in Astrology and Science. *Matrix Journal,* 1992 Summer,

23-38. —1994a. *Astrologie: Hoffnung aufeine Wissenschaft?* [Astrology: Hope of a Science?],

Innsbruck: Resch. An English translation is not available. —1994b. Global Warming or Little Ice Age? Contribution to a festschrift published in

honor of the geologist R. W. Fairbridge in *the Journal of Coastal Research.* Lehman, J. L., 1994. The Mars Diurnal effect: Gauquelin Sectors Meet Classical

Method. *Kosmos,* 22, No. 2 (Spring), 22-46, and simultaneously in *Astrology*

Quarterly, 64/2 Spring 1994, 3-25.

Mandelbrot, M. M., 1983. *The Fractal Geometry of Nature.* New York: W. H. Freeman. Mason, B. I., 1976. Towards the Understanding and Prediction of Climatic Variations.

Quarterly Journal of the Royal Meteorological Society, 102, 478. Mitchell, J. M., C. W. Stockton, and D. M. Meko. 1979. Evidence of a 22-Year Rhythm

of Drought in the Western States Related to the Hale Solar Cycle Since the 17th

Century. In *Solar-Terrestrial Influences on Weather and Climate,* ed. B. M.

McCormac and T. A. Seliga. Dordrecht: D. Reidel, 125-143. Moser, J., 1973. *Stable and Random Motions in Dynamical Systems.* Princeton

University Press. Peixoto, J. P., and A. H. Oort. 1992. *Physics of Climate.* New York: American Institute of

Physics.

Poke, N., 1994. Social Dynamics and the Investment Cycle. *Cycles,* 45, 5, 256. Schneider-Gauquelin, F., 1993. The Planetary Effect in Ordinary People. *Correlation,* 12

(2), Winter 1993/1994, 16-19.

rhumshim, W., 1975. *Unsere innere Uhr.* Zurich: Schweizer Verlaghaus. Winfree A. T., *1987. The Timing of Biological Clocks.* New York: Freeman.